IEICE TRANS. FUNDAMENTALS, VOL. E81–A, NO. 3 MARCH 1998

PAPER

Bifurcations of Periodic Solutions in a Coupled Oscillator with Voltage Ports

Hiroyuki KITAJIMA†, ***Student Member,*** **Yuji KATSUTA**††, ***and*** **Hiroshi KAWAKAMI**†, ***Members***

SUMMARY In this paper, we study bifurcations of equilibrium points and periodic solutions observed in a resistively coupled oscillator with voltage ports. We classify equilibrium points and periodic solutions into four and eight different types, respectively, according to their symmetrical properties. By calculating D-type of branching sets (symmetry-breaking bifurcations) of equilibrium points and periodic solutions, we show that all types of equilibrium points and periodic solutions are systematically found. Possible oscillations in two coupled oscillators are presented by calculating Hopf bifurcation sets of equilibrium points. A parameter region in which chaotic oscillations exist is also shown by obtaining a cascade of period-doubling bifurcation sets.

key words: *bifurcation, symmetry, coupled system, nonlinear circuit*

1. Introduction

Systems of coupled oscillators are good models for biological rhythmic oscillation such as human circadian rhythms [1], finger movements [2], animal locomotion [3], [4] and so on. The investigators have studied the mechanism of oscillation and phase transitions between distinct oscillatory modes. From the standpoint of bifurcation, the former and the latter correspond to Hopf bifurcation of an equilibrium point and D-type of branching of a periodic solution, respectively.

Using group theory, it has been possible to derive some general theorems concerning with the bifurcations of equilibrium points [5], [6]. Papy et al. classified equilibrium points and periodic solutions observed in hybridly coupled two oscillators according to their symmetrical properties [7], [8]. The equilibrium points are completely classified, however the classification of the periodic solutions is not enough, because they treated the periodic solutions with different symmetrical properties as same type. We think that two coupled oscillators' case is a prototype of modeling to understand the phenomena in a large number of coupled oscillators [9], especially even number of coupled oscillators. By obtaining bifurcation diagrams of a system of coupled oscillators we can design the system with the optimal operating condition.

Manuscript received July, 28, 1997.

Manuscript revised November 6, 1997.

†The authors are with the Faculty of Engineering, The University of Tokushima, Tokushima-shi, 770–8506 Japan.

††The author is with Ube National College of Technology, Ube-shi, 755–0031 Japan.

In this paper we investigate bifurcations of equilibrium points and periodic solutions observed in resistively coupled two oscillators with voltage ports. At first we introduce the definition of a symmetrical equation, equilibrium point and periodic solution [10]. Next we classify the periodic solutions according to their symmetrical properties. By calculating bifurcation sets, transitions between the solutions with different symmetrical properties are obtained. Moreover we find chaotic oscillation created by a cascade of period-doubling bifurcations. As far as we know chaotic oscillation is never reported in such a simple coupled system.

2. Circuit Equation

We consider a system of coupled two identical BVP oscillators by a linear resistor with voltage ports, see Fig. 1. The circuit equations are described as

$$\begin{aligned} C\frac{dv_1}{d\tau} &= -g(v_1) - i_1 - G(v_1 - v_2) \\ L\frac{di_1}{d\tau} &= v_1 - ri_1 \\ C\frac{dv_2}{d\tau} &= -g(v_2) - i_2 - G(v_2 - v_1) \\ L\frac{di_2}{d\tau} &= v_2 - ri_2 \end{aligned} \tag{1}$$

where the nonlinear conductance $g(v)$ is assumed to be

$$g(v) = -a_1 v + a_3 v^3. \tag{2}$$

Rescaling coordinate system

$$x_i = \sqrt{L} i_i,\ y_i = \sqrt{C} v_i,\ (i = 1, 2) \tag{3}$$

and changing parameters

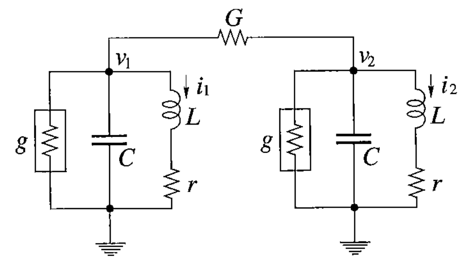

Fig. 1 Oscillator circuit coupled by a resistor.

$$\omega = \frac{1}{\sqrt{LC}}, \ \epsilon = \frac{a_1}{C}, \ \beta = \frac{a_3}{a_1 C}, \ \sigma = \frac{r}{L}, \ \delta = \frac{G}{C} \quad (4)$$

lead to

$$\begin{aligned} \frac{dx_1}{dt} &= \omega y_1 - \sigma x_1 \\ \frac{dy_1}{dt} &= -\omega x_1 + \epsilon(1 - \beta y_1^2) y_1 - \delta(y_1 - y_2) \\ \frac{dx_2}{dt} &= \omega y_2 - \sigma x_2 \\ \frac{dy_2}{dt} &= -\omega x_2 + \epsilon(1 - \beta y_2^2) y_2 - \delta(y_2 - y_1). \end{aligned} \quad (5)$$

By taking the new coordinate system

$$\begin{aligned} r_1 &= \frac{1}{\sqrt{2}}(x_1 + x_2), \quad s_1 = \frac{1}{\sqrt{2}}(y_1 + y_2) \\ r_2 &= \frac{1}{\sqrt{2}}(x_1 - x_2), \quad s_2 = \frac{1}{\sqrt{2}}(y_1 - y_2) \end{aligned} \quad (6)$$

we obtain following equations:

$$\begin{aligned} \frac{dr_1}{dt} &= \omega s_1 - \sigma r_1 \\ \frac{ds_1}{dt} &= -\omega r_1 + \epsilon\left(1 - \frac{\beta}{2}(s_1^2 + 3s_2^2)\right) s_1 \\ \frac{dr_2}{dt} &= \omega s_2 - \sigma r_2 \\ \frac{ds_2}{dt} &= -\omega r_2 + \epsilon\left(1 - \frac{\beta}{2}(s_2^2 + 3s_1^2)\right) s_2 - 2\delta s_2. \end{aligned} \quad (7)$$

3. Definition of Symmetrical Properties

[**Equation**]

Equation (7) can be rewritten as

$$\frac{dx}{dt} = f(x, \lambda) \quad (8)$$

If there exists a matrix P satisfying

$$f(Px, \lambda) = Pf(x, \lambda) \quad (9)$$

then Eq. (8) is called P-symmetrical equation.

[**Equilibrium point**]

We say that an equilibrium point e_0 such that

$$Pe_0 = e_0 \quad (10)$$

is P-invariant equilibrium point.

[**Periodic solution**]

We assume a periodic solution of Eq. (8) with initial condition $x_0 := x(0)$ as

$$x(t) = \varphi(x_0, t). \quad (11)$$

If there exists a matrix P and a time τ_P such that

$$P\varphi(x, t) = \varphi(Px, t) = \varphi(x, t - \tau_P) \quad (12)$$

then we call that the periodic solution $\varphi(x, t)$ is (P, τ_P)-symmetrical periodic solution. The phase difference ϕ between the waveforms of each oscillator is defined by:

$$\phi = 2\pi \frac{\tau_P}{L} \quad (13)$$

where L is the period of the periodic solution. We call solutions in-phase and anti-phase when $\phi = 0$ and $\phi = \pi$, respectively. Thus symmetries of periodic solutions have both a spatial component P and a temporal component τ_P.

Consider Eq. (7), matrices satisfying Eq. (9) are

$$I_4 = \begin{bmatrix} I_2 & O \\ O & I_2 \end{bmatrix}, \quad \sigma_1 = \begin{bmatrix} I_2 & O \\ O & \bar{I}_2 \end{bmatrix}, \quad \sigma_2 = \begin{bmatrix} \bar{I}_2 & O \\ O & I_2 \end{bmatrix}, \quad \bar{I}_4 = \begin{bmatrix} \bar{I}_2 & O \\ O & \bar{I}_2 \end{bmatrix} \quad (14)$$

where I_2 is 2×2 identity matrix, O is 2×2 zero matrix and $\bar{I}_2 = -I_2$. The set Γ:

$$\Gamma = \{I_4, \sigma_1, \sigma_2, \bar{I}_4\} \quad (15)$$

forms an abelian group with the multiplication as shown in Table 1.

Table 1 Group table of Γ.

	I_4	σ_1	σ_2	$\bar{I}_4$
I_4	I_4	σ_1	σ_2	$\bar{I}_4$
σ_1	σ_1	I_4	$\bar{I}_4$	σ_2
σ_2	σ_2	$\bar{I}_4$	I_4	σ_1
$\bar{I}_4$	$\bar{I}_4$	σ_2	σ_1	I_4

4. Results

4.1 Classification of Equilibrium Points and Periodic Solutions

We classify equilibrium points according to their symmetrical properties in Table 2. There exist four kinds of equilibrium points in Eq. (7). Figure 2 shows locations of each equilibrium point in (r_1, s_1) and (r_2, s_2) space. The origin (●) is an equilibrium point with full symmetry Γ. The equilibrium points (■) and (▲) are σ_1- and σ_2-invariant equilibrium points by the definition Eq. (10), respectively. The equilibrium points (×) has only symmetry operation I_4, thus it is asymmetry. When there is an asymmetrical equilibrium point, the orbit of Γ (14) defines immediately three other equilibrium points, see Fig. 2.

By the definition of symmetrical periodic solution, i.e., Eq. (12), we classify periodic solutions observed in Eqs. (7), see Table 3. From this table, we see that in total eight kinds of periodic solutions exist in Eq. (7) (In Ref. [8] they classified periodic solutions into five types). All of them is sketched on (r_1, r_2) plane in Fig. 3. We will use the name written in each sub-caption here.

4.2 Bifurcation of Equilibrium Point

The Jacobian matrix of the system at the equilibrium

Table 2 Classification of equilibrium points (abbrev. EP) according to their symmetrical properties.

type (m)	symmetry operation	#EP	symbol
full symmetry (0)	$\{I_4, \sigma_1, \sigma_2, \bar{I}_4\}$	1	●
σ_1-invariant (1)	$\{I_4, \sigma_1\}$	2	■
σ_2-invariant (2)	$\{I_4, \sigma_2\}$	2	▲
asymmetry	$\{I_4\}$	4	×

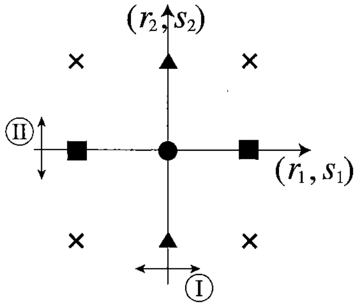

Fig. 2 Classification of equilibrium points according to their symmetrical properties. Symbols are referred to Table 2. Axes (r_i, s_i) represent subspace satisfying $\sigma_i x = x$ where $x = (r_1, s_1, r_2, s_2)$ called σ_i-invariant subspace ($i = 1, 2$). The origin is invariant under coordinate transformation by σ_1, σ_2 and $\bar{I}_4$.

Table 3 Classification of periodic solutions (abbrev. PS) according to their symmetrical properties.

symmetries	#PS	comment
$(\sigma_1, 0), (\sigma_2, L/2), (\bar{I}_4, L/2)$	1	in-phase
$(\sigma_2, 0), (\sigma_1, L/2), (\bar{I}_4, L/2)$	1	anti-phase
$(\sigma_1, 0)$	2	"shifted" in-phase
$(\sigma_2, 0)$	2	"shifted" anti-phase
$(\sigma_2, L/2)$	2	almost in-phase
$(\sigma_1, L/2)$	2	almost anti-phase
$(\bar{I}_4, L/2)$	2	$\bar{I}_4$-invariant
$(I_4, 0)$	4	asymmetry

point $(r_{10}, s_{10}, r_{20}, s_{20})$ [11] is

$$J = \begin{bmatrix} -\sigma & \omega & 0 & 0 \\ -\omega & \epsilon\left(1 - \frac{3\beta}{2}(s_{10}^2 + s_{20}^2)\right) & 0 & -3\epsilon\beta s_{10}s_{20} \\ 0 & 0 & -\sigma & \omega \\ 0 & -3\epsilon\beta s_{10}s_{20} & -\omega & \epsilon\left(1 - \frac{3\beta}{2}(s_{10}^2 + s_{20}^2)\right) - 2\delta \end{bmatrix} \tag{16}$$

Parameters in Eq. (7) are fixed as

$$\sigma = 0.8,\ \beta = 1.0,\ \omega = 1.0. \tag{17}$$

We investigate bifurcation problems in the (δ, ϵ) parameter plane. By calculating the eigenvalues μ of Eq. (16),

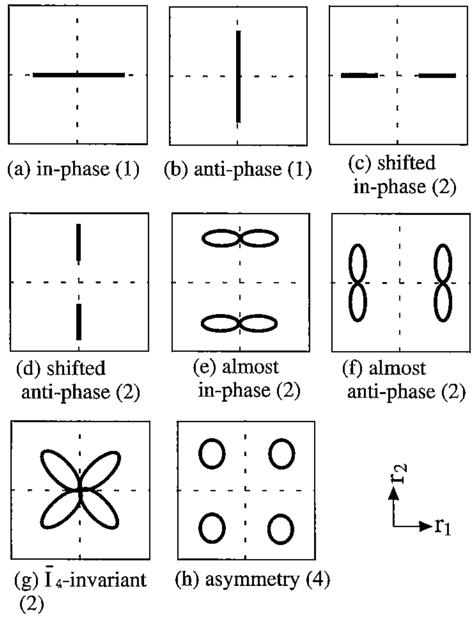

Fig. 3 Classification of periodic solutions. Parenthesized number indicates number of periodic solutions corresponding to #PS in Table 3.

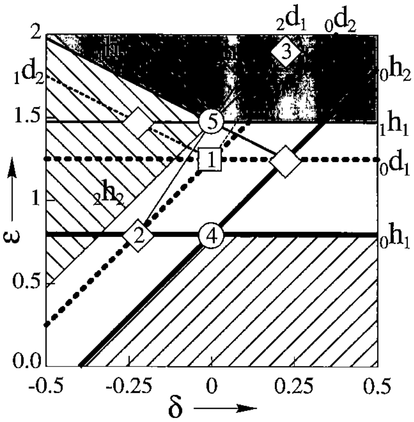

Fig. 4 Bifurcation diagram of equilibrium points. Solid lines (h) and dashed lines (d) indicate Hopf bifurcation set and D-type of branching set, respectively.

we obtain Hopf bifurcation ($\mu = \pm i\omega$) and D-type of branching ($\mu = 0$) sets. The results are shown in Fig. 4 as a bifurcation diagram.

In Fig. 4 the notations ${}_m\mathrm{h}_k$ and ${}_m\mathrm{d}_k$ indicate, respectively, Hopf bifurcation set and D-type of branching set of type m equilibrium point, see Table 2; k denotes the bifurcating direction (Ⅰ or Ⅱ in Fig. 2). The symbols ○, ◇ and □ represent codimension two, three and four bifurcations which are the points of intersection of double Hopf bifurcations, D-type of branching and Hopf bifurcation, and double D-type of branchings, respectively. In the regions ▨, ▩ and ▧ there exist stable equilibrium points whose type is, respectively, full symmetry, σ_1-invariant and σ_2-invariant.

At first we explain bifurcation structure and stability of equilibrium points around the point marked by [1]. In Sect. 4.3 we will show detailed bifurcation diagrams including bifurcation sets of periodic solutions around the points marked by ◇2, ◇3, ④ and ⑤.

Figure 5 shows only D-type of branching sets in Fig. 4. A schematic bifurcation diagram is shown in Fig. 6 when the parameters ϵ and δ change along the curve l in Fig. 5. In Fig. 6 from the points marked by ①, ②, ⑤ and ⑥ "two" equilibrium points are generated by D-type of branching, but we omit one of them because two branches have same bifurcation structure. From Fig. 6, we see that there exist one equilibrium point with full symmetry in whole parameter plane, two σ_2-invariant equilibrium points between ① and ⑤, two σ_1-invariant equilibrium points between ② and ⑥, and four equilibrium points without symmetry between ③ and ④. Since the equilibrium point with full symmetry is already completely unstable (${}_4O$) by two Hopf bifurcations ${}_0h_1$ and ${}_0h_2$, equilibrium points generated by D-type of branchings (${}_0d_1$, ${}_0d_2$, ${}_1d_2$ and ${}_2d_1$) are all unstable.

In Table 4 we show that Hopf bifurcations in Fig. 4 generate what kind of periodic solutions. From this table we see that six kinds of periodic solutions are generated by Hopf bifurcations of three kinds of equilibrium points and "$\tilde{I}_4$-invariant" periodic solution never appear by Hopf bifurcation.

4.3 Bifurcation of Periodic Solution

We show in Fig. 7 a bifurcation diagram around the point marked by ◇2 in Fig. 4 (the point of intersection of D-type of branching set ${}_0d_2$ and Hopf bifurcation set ${}_0h_1$). Figure 8 shows a bifurcation diagram when the parameters change along the curve l in Fig. 7. "Almost in-phase" solutions generated by D-type of branching D_3 (③) of in-phase solution meet Neimark-Sacker bifurcation N (④) and disappear by the Hopf bifurcation ${}_2h_1$ (⑤) of σ_2-invariant equilibrium points.

Figure 9 shows a bifurcation diagram around the point marked by ◇3 in Fig. 4 (the intersection point of ${}_2d_1$ and ${}_2h_2$). In small parameter region there exist many bifurcation sets and the bifurcation diagram becomes complicated therefore we use a schematic dia-

Table 4 Hopf bifurcations of equilibrium points shown in Fig. 4.

notation	bifurcation
${}_0h_1$	full symmetry ⇔ in-phase
${}_0h_2$	full symmetry ⇔ anti-phase
${}_1h_1$	σ_1-invariant ⇔ "shifted" in-phase
${}_1h_2$	σ_1-invariant ⇔ almost anti-phase
${}_2h_1$	σ_2-invariant ⇔ almost in-phase
${}_2h_2$	σ_2-invariant ⇔ "shifted" anti-phase

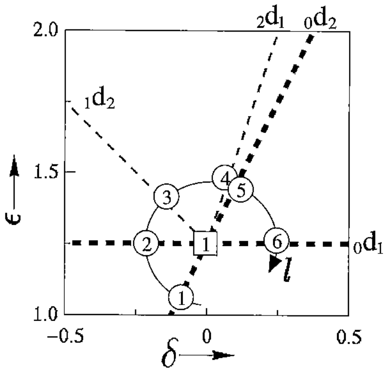

Fig. 5 Bifurcation diagram around the intersection point of double D-type of branchings.

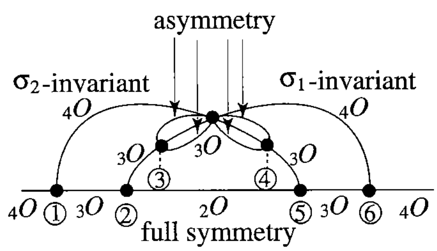

Fig. 6 Bifurcation diagram corresponding to the curve l in Fig. 5. The symbol O indicates equilibrium point and its subscript represents a dimension of unstable subspace.

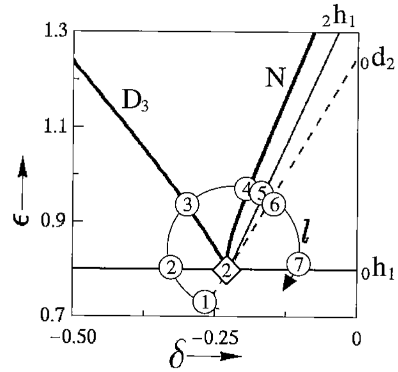

Fig. 7 Bifurcation diagram around the intersection point of Hopf bifurcation and D-type of branching. N represents Neimark-Sacker bifurcation.

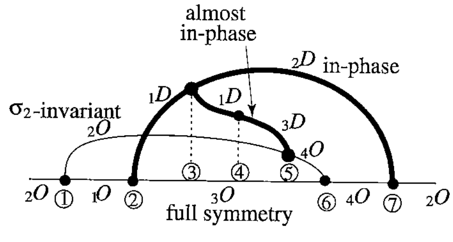

Fig. 8 Bifurcation diagram corresponding to the curve l in Fig. 7. Heavy curves (D) and light curves (O) indicate periodic solutions and equilibrium points, respectively. Subscripts of D and O represent a dimension of unstable subspace.

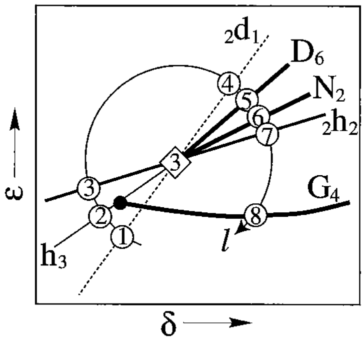

Fig. 9 Schematic bifurcation diagram around the intersection point of Hopf bifurcation and D-type of branching.

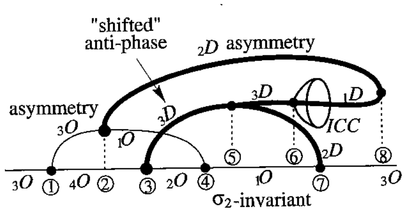

Fig. 10 Bifurcation diagram corresponding to the curve l in Fig. 9.

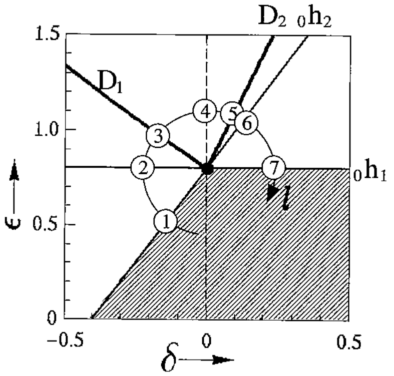

Fig. 11 Bifurcation diagram around the intersection point of double Hopf bifurcations. D represents D-type of branching of periodic solution.

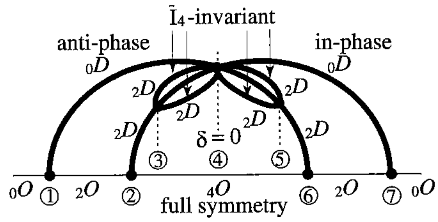

Fig. 12 Bifurcation diagram corresponding to the curve l in Fig. 11.

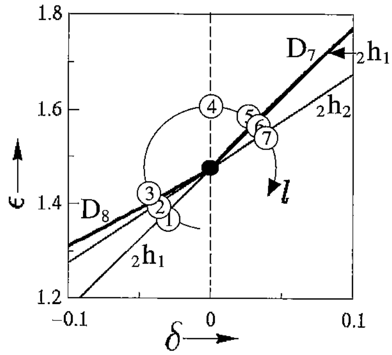

Fig. 13 Bifurcation diagram around the intersection point of double Hopf bifurcations.

gram. Figure 10 shows a bifurcation diagram when the parameters change along the curve l in Fig. 9. Bifurcation structure is similar to that of Fig. 7, but in Fig. 9 there exists tangent bifurcation set G_4 and asymmetrical solution is folded (the point marked by ⑧ in Fig. 10). Four unstable ICCs (Invariant Closed Curves) which correspond to quasi-periodic solutions are generated by N_2 (⑥). Those results permit us to predict that similar bifurcation structure would exist around the points marked by ◇ in Fig. 4.

We show in Fig. 11 a bifurcation diagram around the point marked by ④ in Fig. 4 (the intersection point of $_0h_1$ and $_0h_2$). In the shaded region ▨, one stable equilibrium point with full symmetry exists. From this region increasing the parameter ϵ and crossing $_0h_1$, we obtain a stable in-phase solution. On the other hand decreasing the parameter δ and crossing $_0h_2$, a stable anti-phase solution appears. Figure 12 shows a bifurcation diagram when the parameters change along the curve l in Fig. 11. The in-phase and the anti-phase solution appeared at ②, ⑦ and ①, ⑥, respectively, generate "$\bar{I}_4$-invariant" periodic solutions by D-type of branchings D_1 (③) and D_2 (⑤). On the axis of $\delta = 0$, the dimension of unstable subspace is changed through a cusp point.

We show in Fig. 13 a bifurcation diagram around the point marked by ⑤ in Fig. 4 (the intersection point of $_2h_1$ and $_2h_2$ and also of $_1h_1$ and $_1h_2$). Bifurcation structure is the same as that of Fig. 11, but symmetrical properties and stability are changed, see Fig. 14.

Figure 15 shows a bifurcation diagram in the large value of parameter ϵ. The in-phase solution and the anti-phase solution generated by the Hopf bifurcations $_0h_1$ and $_0h_2$ disappear by tangent bifurcations G_1 and G_2, respectively [12]. "$\bar{I}_4$-invariant" periodic solutions caused by D_1 of the in-phase solution and D_2 of the anti-phase solution meet D_4 and generate four asymmetrical solutions. Figure 16 shows a bifurcation diagram of the asymmetrical solutions. Inside period-doubling bifurcation set I_1 there is a cascade of period-doubling bifurcations and asymmetrical chaotic state appears, see Fig. 17. From Fig. 17 (b), this chaotic attractor has any symmetry operations therefore in total four chaotic attractors exist. In a system of coupled two oscillators where the single oscillator does not have any chaotic oscillations, the existence of stable asymmetry periodic

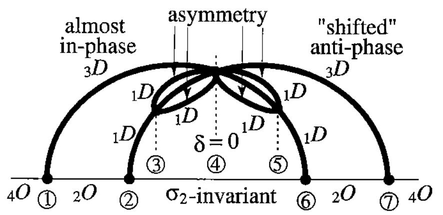

Fig. 14 Bifurcation diagram corresponding to the curve l in Fig. 13.

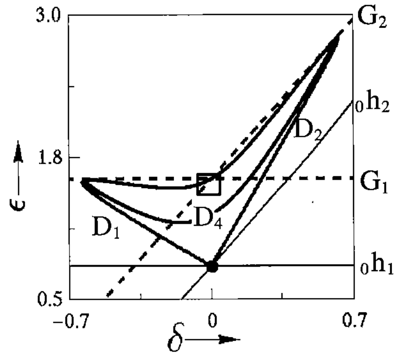

Fig. 15 Bifurcation diagram of in-phase and anti-phase solution.

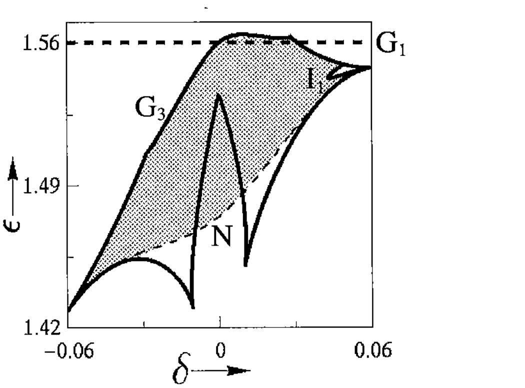

Fig. 16 Enlarged diagram of Fig. 15. In the shaded region ▒ the asymmetrical solutions stably exist.

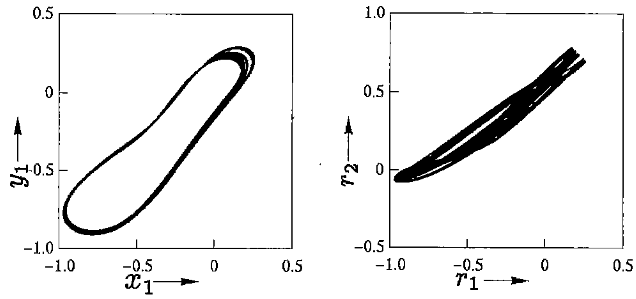

(a) (x_1, y_1) plane. (b) (r_1, r_2) plane.

Fig. 17 Chaotic attractor. $\alpha = 1.546$, $\delta = 0.05$.

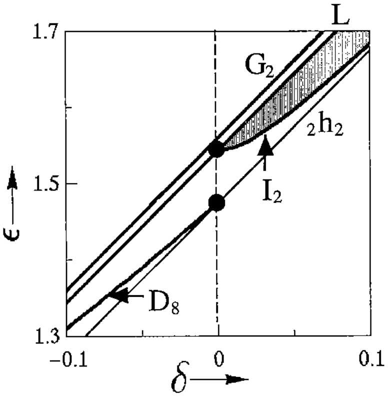

Fig. 18 Bifurcation diagram of "shifted anti-phase" solution created by Hopf bifurcation set $_2h_2$. The curve L denotes a global bifurcation set.

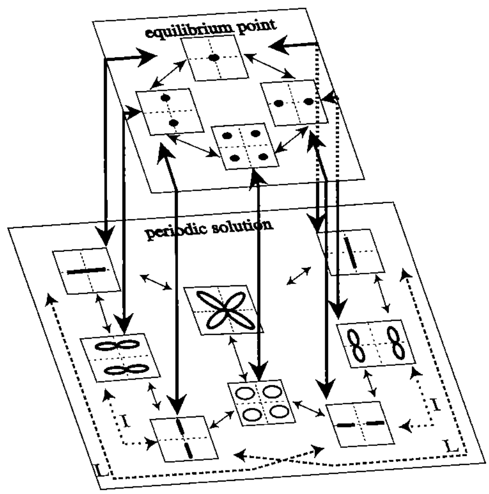

Fig. 19 Possible symmetry-breaking bifurcations observed in Eq. (7). Small squares represent (r_1, r_2) phase plane. Heavy and light solid lines indicate Hopf bifurcation and D-type of branching, respectively. The dotted lines I and the dashed lines L indicates period-doubling bifurcations and global bifurcations, respectively.

solution is one of the most important condition for existing a chaotic attractor.

Figure 18 shows a detailed bifurcation diagram of Fig. 13. In the shaded region ▒, there exist "almost in-phase" 2-periodic solutions generated by period-doubling bifurcation set I_2 of "shifted anti-phase" solution. By crossing the L, two "shifted anti-phase" solutions bifurcate to one anti-phase solution after separatrix loops.

In Fig. 19 we summarize the results obtained from calculating the bifurcation sets of equilibrium points and periodic solutions in Eqs. (7).

5. Conclusions

We investigated bifurcations of equilibrium points and periodic solutions observed in a resistively coupled oscillator with voltage ports. Firstly we classified theoretically all equilibrium points and periodic solutions according to their symmetrical properties. Eight types of periodic solutions including in-phase and anti-phase solutions [14] were shown. Secondly by calculating bifurcation sets numerically we demonstrated the existence of the equilibrium points and the periodic solutions which we classified. Lastly we showed transitions of solutions between different types of symmetries by symmetry-breaking bifurcation. Moreover we found chaotic oscillation created by successive period-doubling bifurcations. As far as we know, this is the first observation of chaotic oscillation in such a simple coupled oscillators system.

Extension to large number of oscillators and calculation of global bifurcation sets are interesting problems for the future.

Acknowledgement

This work is partially supported by the Grant-in-Aid for JSPS Fellow (No. 1510) from the Ministry of Education, Science, Sports, and Culture of Japan.

References

[1] T. Yoshinaga and H. Kawakami, "Bifurcations in coupled BVP equations with forcing term," Proc. ISCAS'91, vol.5-5, pp.2697–2700, June 1991.
[2] T. Hirao, H. Nagashino, and Y. Kinouchi, "Recruitment and annihilation of the oscillatory activities in coupled neural oscillators," Proc. NOLTA'96, pp.5–8, Kouchi, Japan, Oct. 1996.
[3] T. Ikemoto, H. Nagashino, Y. Kinouchi, and T. Yoshinaga, "Transitions of oscillation modes in a four coupled neural oscillator model with reciprocal inhibition," IEICE Technical Report, NLP97-36, May 1997.
[4] J.J. Collins and I. Stewart, "Coupled nonlinear oscillators and the symmetries of animal gaits," J. Nonlinear Science, vol.3, pp.349–392, Springer-Verlag, New York, 1993.
[5] M. Golubitsky and D.G. Schaeffer, "Singularities and Groups in Bifurcation Theory," vol.I, Springer-Verlag, New York 1985.
[6] M. Golubitsky, I. Stewart, and D.G. Schaeffer, "Singularities and Groups in Bifurcation Theory," vol.II, Springer-Verlag, New York 1988.
[7] O. Papy and H. Kawakami, "Symmetrical properties and bifurcations of the equilibria for a resistively coupled oscillator with hybrid connection," IEICE Trans. Fundamentals, vol.E78-A, no.12, pp.1822–1827, Dec. 1995.
[8] O. Papy and H. Kawakami, "Symmetrical properties and bifurcations of the periodic solutions for a hybrid coupled oscillator," IEICE Trans. Fundamentals, vol.E78-A, no.12, pp.1816–1821, Dec. 1995.
[9] T. Endo and S. Mori, "Mode analysis of a ring of a large number of mutually coupled van der Pol oscillators," IEEE Trans. Circuit & Syst., vol.CAS-25, no.1, pp.7–18, Jan. 1978.
[10] Y. Katsuta and H. Kawakami, "Bifurcations of equilibriums and periodic solutions in nonlinear autonomous system with symmetry," IEICE Trans., vol.J75-A, no.6, pp.1035–1044, June 1992.
[11] H. Kitajima, Y. Noumi, Y. Katsuta, and H. Kawakami, "Bifurcation of periodic solutions in a coupled oscillator with voltage ports," IEICE Technical Report, NLP97-1, May 1997.
[12] A.N. Bautin, "Qualitative investigation of a particular nonlinear system," PPM, vol.39, no.4, pp.606–615, 1975.
[13] Y. Noumi and H. Kawakami, "Forced synchronization of coupled oscillators," IEICE Technical Report, NLP96-172, March 1997.
[14] T. Suezaki and S. Mori, "Mutual synchronization of two oscillators," IECE, vol.48, no.9, pp.1551–1557, Sept. 1965.

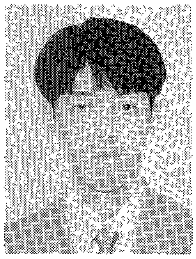

Hiroyuki Kitajima was born in Tokushima, Japan, on June 25, 1970. He received the B.Eng. and M.Eng. degrees in Electrical and Electronic Engineering from Tokushima University, in 1993 and 1995 respectively. He is a Research Fellow of the Japan Society for the Promotion of Science and presently working toward the Ph.D. degree at Tokushima University. He is interested in bifurcation problems.

Yuji Katsuta graduated in 1980 from the Department of Electronic Engineering, Tokushima University, where he received his Master's degree in 1982, and affiliated with Sharp Corporation. Later, he received his Dr. of Eng. degree. He was a Lecturer in 1990 and an Associate Professor in 1994 in the Department of Intelligent System Engineering, Ube National College of Technology. He is interested in nonlinear problems.

Hiroshi Kawakami was born in Tokushima, Japan, on December 6, 1941. He received the B.Eng. from Tokushima University, Tokushima, Japan, in 1964, the M.Eng. and Dr.Eng. degrees from Kyoto University, Kyoto, Japan, in 1966 and 1974, respectively, all in electrical engineering. Presently, he is Professor of Electrical and Electronic Engineering, Tokushima University, Tokushima, Japan. His interest is qualitative properties of nonlinear circuits.